DYNAMIC COMPRESSIVE RESPONSE OF COMPOSITE SQUARE HONEYCOMBS

S. Park*, B.P. Russell, V.S. Deshpande, N.A. Fleck
Engineering Department, University of Cambridge
Trumpington Street, Cambridge CB2 1PZ, United Kingdom
* S. Park (sp506@cam.ac.uk)

Keywords: *honeycomb cores, carbon fibre, composites, impact testing, rate dependence*

1 Introduction

Long fibre polymer matrix composites are finding increasing application due to their superior strength-to-density ratio compared with traditional metals. Composites are promising candidates as materials for low density core design for use in sandwich constructions.

Recently, composite square honeycomb lattices [1] have been fabricated and their performance evaluated under quasi-static loading. Superior strength was observed in these novel materials when compared with their metallic equivalents. However, the dynamic response of sandwich panels with composite lattice core topologies is little understood. Scenarios such as bird-strike or blast mitigation motivate this study.

Recent studies on metallic honeycombs have revealed that square honeycomb cores have good crushing resistance and energy absorption under shock loading [2, 3, 4]. These results suggest that square honeycomb topology has a good potential as a core material for sandwich panel under a dynamic loading scenario.

This study aims to experimentally investigate the dynamic compressive response of the square honeycomb fabricated from carbon-fibre/epoxy composite material.

2 Materials and manufacturing process

The manufacturing process of composite square honeycomb follows the one developed by Russell et al. [1]. As shown in Fig. 1, composite honeycombs have been manufactured from cured composite sheets of 2x2 twill weave architecture made from T300-6K carbon fibre tows embedded in an epoxy matrix (Fiberite 934). The cured composite sheet has a density of 1370 kgm^{-3}. The relative density of the square honeycomb is given by

$$\bar{\rho} \approx \frac{2t}{L} \tag{1}$$

where L is the cell spacing. To achieve honeycombs of relative densities of 0.12 and 0.24, the parameter L was varied and the sheet thickness was held fixed at 0.355 mm for all honeycombs.

The cured composite sheet was machined into slotted strips of height H, width W, and cell spacing L using 2 axis micro-milling machine. The number of cells and the detailed dimensions of different relative density honeycombs are shown in Table 1. The fibre tows investigated in this study have been cut to be oriented at 0/90° with respect to loading direction. The cell aspect ratio $H/L = 3$ has been kept constant regardless of relative densities. The slotted strips have been assembled and low viscosity epoxy resin has been applied to the joins. The whole assembly was then cured at 65 °C for one hour.

3 Quasi-static investigation

The understanding of failure mechanisms under quasi-static loading is crucial in the analysis of the dynamic behaviour of honeycombs under high strain-rate loading. Quasi-static compression tests have been conducted on a screw driven test machine (Instron 5584) at an applied nominal strain rate $\dot{\varepsilon} = 10^{-3}\,\mathrm{s}^{-1}$ with the nominal stress inferred from the load cell of test machine and the axial strain inferred

from a laser extensometer using a gauge length equal to that of the specimen height.

The parent material properties can be found in Russell et al. [1].

The deformation history of honeycombs for two different relative densities is shown in Fig. 2. The peak failure strength from this experiment agrees well with the results from Russell et al. [1] who performed compression tests on nearly identical specimens where the honeycombs were bonded to face sheets (thus preventing the occurrence of edge damage). They [1] have also shown from analytical expressions that the honeycomb geometries discussed in this paper would fail by plastic microbuckling. This is supported by Fig. 2 which shows that both relative density honeycombs start yielding at the similar wall stress level.

4 Dynamic investigation

4.1 Dynamic experimental setup

The dynamic experimental setup is shown in Fig. 3. This setup follows closely that developed by Radford et al. [4]. The steel strikers accelerated by means of a gas gun were used to crush the honeycomb specimen. The mass of the striker was chosen such that the specimen was crushed with a constant crush velocity. Four striker velocities were used: $v_0 = 25$, 50, 100, 150 ms^{-1}. For the $\bar{\rho} = 0.12$ honeycomb (where H = 17.75 mm), these result in strain rates of 1400, 2800, 5500 and 8300 s^{-1}, and for $\bar{\rho} = 0.24$ (H = 8.875 mm), these result in strain rates of 2800, 5500, 11000 and 16500 s^{-1}.

The honeycomb specimens have been located in two different (front face and back face) configurations to measure the stresses induced in different faces. In the front face configuration, the honeycomb specimen was attached to the striker and accelerated together to impact on the Kolsky bar, enabling measurement of the stresses induced in the front face. In the back face configuration, the honeycomb specimen was attached to the stationary Kolsky bar and the striker impacts the front face of the specimen, enabling measurement of the stresses induced at back face of the specimen.

The maraging steel (M-300) Kolsky bar with length of 2.2 m and diameter of 28.5 mm was instrumented by two 1 mm strain gauges mounted diametrically opposite each other at a distance of 10 diameters from the impact end. The strain gauges were wired in the half-Wheatstone bridge configuration, and the signal recorded on a digital oscilloscope via an amplifier with a cut-off frequency of 500 kHz. The force transmitted to the Kolsky bar from the test specimens was inferred from the strain measurement. Calibration test has been conducted to ensure the accuracy of the setup and the system has been ensured to give out predicted theoretical stress output by firing known velocity striker. The response time of the system during calibration test, i.e. the time taken to reach peak stress, was recorded as 15 μs.

During dynamic tests, high speed camera (Phantom V12) has been used simultaneously to capture the images of dynamic deformation of the honeycombs. High speed images have been captured with interframe time of 3.7 μs and exposure time of 0.7 μs.

4.2 Dynamic response of honeycombs

The dynamic deformation history is shown in Fig. 4 for two chosen velocities $v_0 = 25$ and 150 ms^{-1} with high speed images shown in Fig. 5. Figure 4 shows that dynamic strength enhancement is achieved when compared with quasi-static response of honeycombs. In all cases but one, the front and back face stresses are similar. This indicates that these specimens are in axial equilibrium. The exception is $\bar{\rho} = 0.12$ specimen loaded at $v_0 = 150$ ms^{-1} which shows a higher front face stress, thus indicating this specimen is not in axial equilibrium. This is shown clearly in Fig. 6 where a separation of front and back face peak stresses are seen at impact velocities $v_0 \geq 100$ ms^{-1}.

In Fig. 6, the peak strength of dynamic stress curve of honeycombs have been normalised by the quasi-static failure strength of parent material (370 MPa) and plotted against strain rate.

Dynamic strength enhancement of both honeycomb geometries can be attributed to material strain-rate sensitivity. Both relative density honeycombs failed by plastic microbuckling under quasi-static loading. The strength enhancement in the material is likely to be either material strain-rate sensitivity of epoxy or buckling stabilisation of the fibres, both of which would lead to micro inertial stabilisation effect of the plastic microbuckle.

6 Concluding remarks

The composite honeycomb has been manufactured from the cured composite sheets by slotting, assembling and curing. Two relative densities of honeycombs have been manufactured by varying the cell size. These honeycombs have been tested under quasi-static and dynamic compression.

Under quasi-static compression, both relative density honeycombs fail by microbuckling. Under dynamic loading, the honeycombs show dynamic strength enhancement as the impact velocity increases. This dynamic strength enhancement is attributed to micro inertial stabilisation of the plastic microbuckle. The $\bar{\rho} = 0.12$ honeycombs are not in axial equilibrium at impact velocities $v_0 \geq 100\ \mathrm{ms}^{-1}$.

Table 1: Dimensions of the specimen manufactured in this study. All dimensions are in mm.

$\bar{\rho}$	Cells	W	H	L	t
0.12	3 x 3	20.15	17.76	5.92	0.355
0.24	6 x 6	20.15	8.88	2.96	0.355

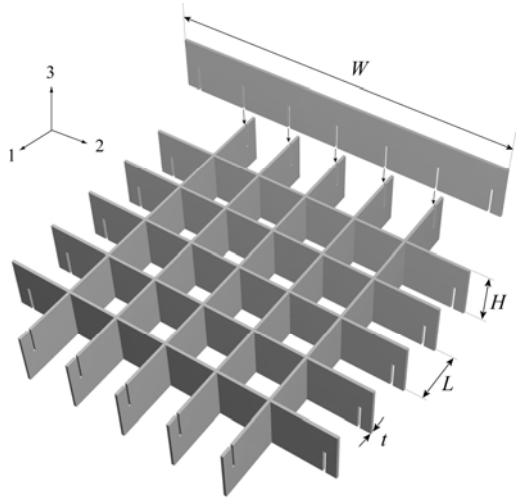

Fig. 1. Square honeycomb manufacturing technique.

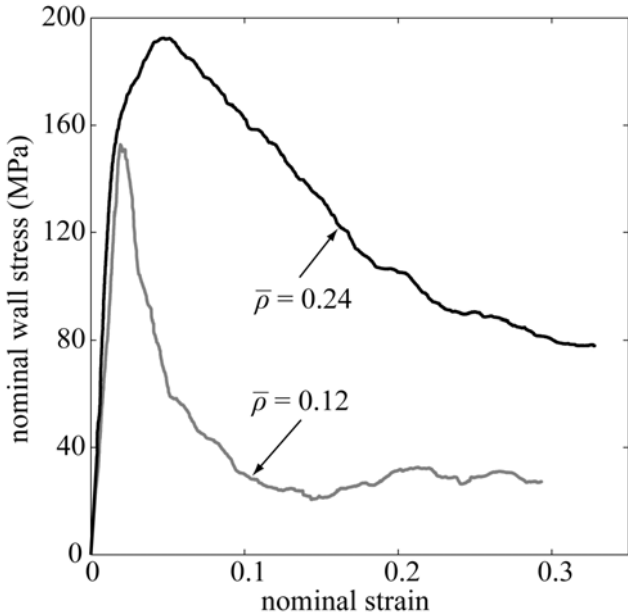

Fig. 2. Quasi-static compressive response of square honeycombs with two different relative densities, $\bar{\rho} = 0.12$ and 0.24.

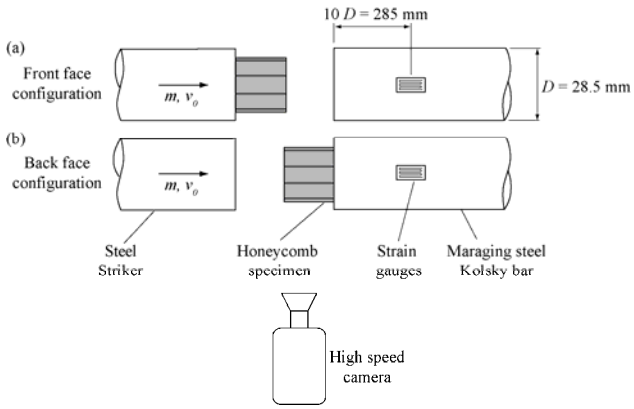

Fig. 3. Dynamic test setup showing (a) front face configuration and (b) back face configuration.

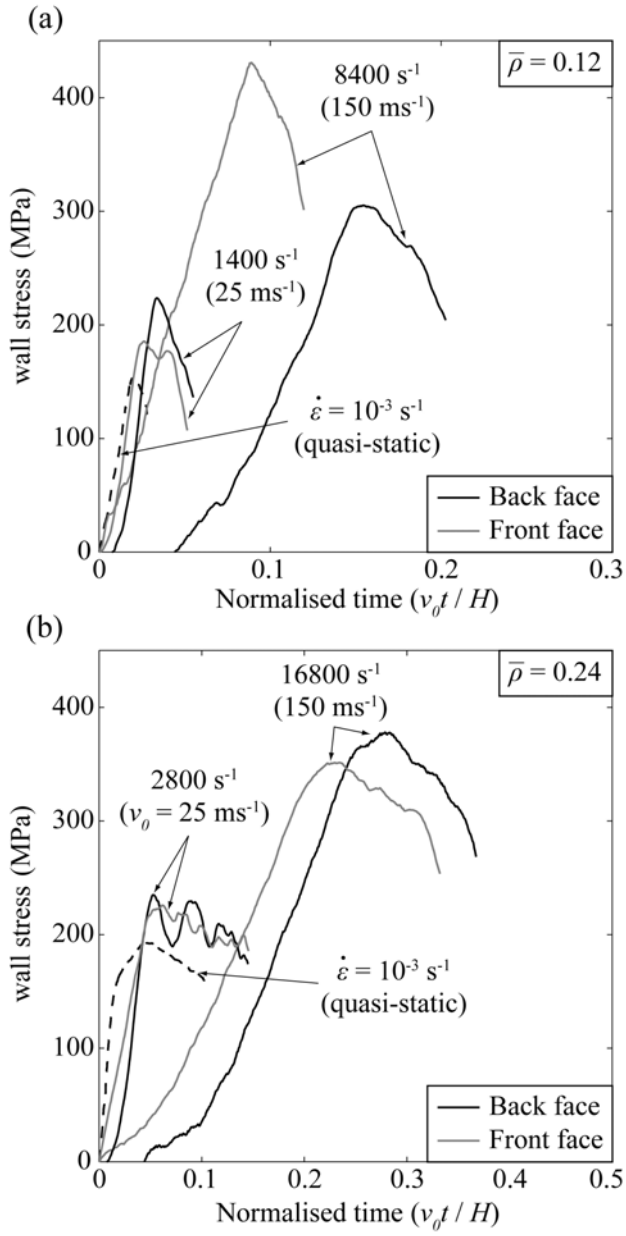

Fig. 4. Dynamic compressive response of square honeycombs with two different relative densities (a) $\bar{\rho} = 0.12$ and (b) $\bar{\rho} = 0.24$ for two different velocities $v_0 = 25{,}150$ ms^{-1}.

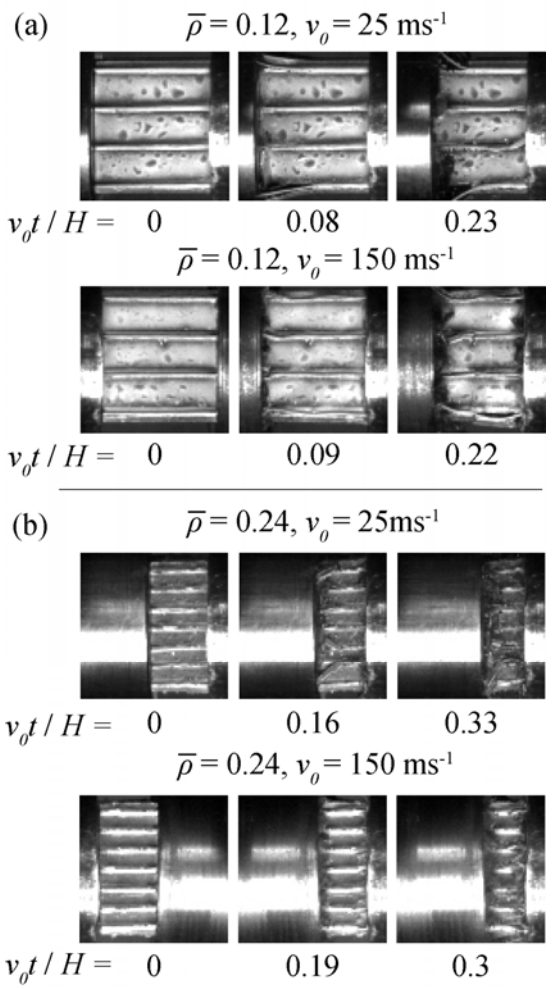

Fig. 5. High speed images of dynamic deformation of composite square honeycomb with relative densities (a) $\bar{\rho} = 0.12$ and (b) $\bar{\rho} = 0.24$ with corresponding strain from impact.

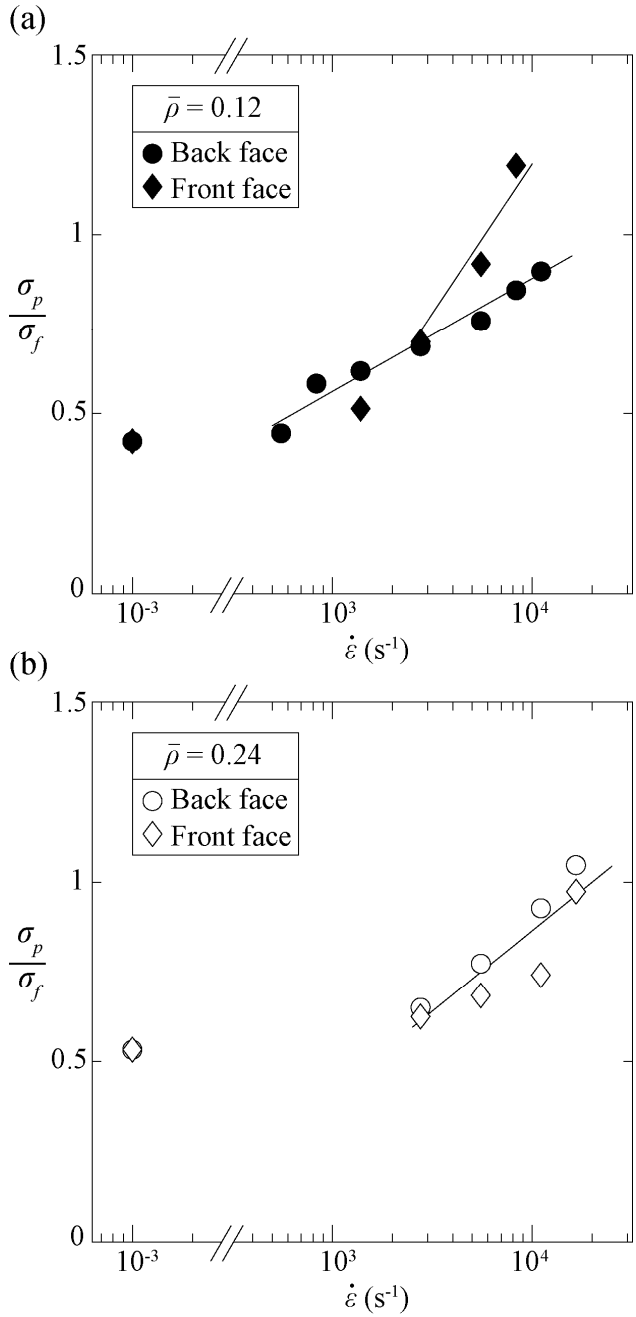

Fig. 6. Summary of normalized peak strength of dynamic stress measurements of different relative density honeycombs (a) $\bar{\rho} = 0.12$ and (b) $\bar{\rho} = 0.24$ tested in this study.

References

[1] B.P. Russell, V.S. Deshpande, and H.N.G. Wadley, "Quasistatic deformation and failure modes of

composite square honeycombs," *J. Mech. and Struc.*, vol.3, no.7, pp. 1315-1340, 2008.

[2] Z. Xue, and J.W. Hutchinson, "A comparative study of blast-resistant metal sandwich plates," *Int. J. Impact Eng.*, 30, pp. 1283-1305, 2004.

[3] N.A. Fleck, and V.S. Deshpande, "The resistance of clamped sandwich beams to shock loading," *J. Appl. Mech.*, 71, pp. 286-401, 2004.

[4] D.D. Radford, G.J. McShane, V.S. Deshpande, and N.A. Fleck, "Dynamic compressive response of stainless-steel square honeycombs," *J. Appl. Mech.*, 74, pp. 658-667, 2007.